Journal of Applied Fluid Mechanics, Vol. 10, No. 6, pp. 1679-1688, 2017.
Available online at www.jafmonline.net, ISSN 1735-3572, EISSN 1735-3645.
DOI: 10.29252/jafm.73.245.27878

Experimental Investigation of Tip Vortex Meandering in the Near Wake of a Horizontal-Axis Wind Turbine

A. W. Dahmouni [1†], M. M. Oueslati [1] and S. Ben Nasrallah [2]

[1] *Laboratory of Wind Power Control and Energy Valorization of Waste (LMEEVED), Research and Technology Center of Energy (CRTEn), BP 95 Hammam Lif 2050, Tunisia.*
[2] *Laboratory of Thermal and Energy Systems Studies (LESTE), National Engineering School of Monastir, Monastir 5019, Tunisia.*

†*Corresponding Author Email: dahmouni_anouar_wajdi@yahoo.fr*

(Received April 15, 2017; accepted May 13, 2017)

ABSTRACT

The aerodynamic optimization of horizontal axis wind turbine has became one of the most important challenge in the renewable energy field. Over the past few years, many researchers have drawn more attention to the physical processes of the wind energy conversion and precisely the identification of the main causes of energy losses. This paper presents an experimental investigation of near wake dynamics for a model horizontal axis wind turbine in a wind tunnel. The coherent structures downstream of the rotor were studied for different tip speed ratios using the Particle Image Velocimetry (PIV) technique. The influence of the tip vortex meandering was discussed and analyzed using the Proper Orthogonal Decomposition (POD) method. The high-energy modes show that radial meandering is the most energetic source of perturbation in each tip vortex sub-region. The energy fraction of these modes increase gradually during the development of the helical tip vortex filament, which confirm the growth of vortex wandering amplitude in the near wake.

Keywords: Wind turbine; Near wake; Tip vortex; Meandering; POD.

NOMENCLATURE

a_n	POD coefficients	V	wind speed velocity
c	blade cord	v	radial velocity
C_{nm}	spatial correlation matrix	x, y, z	cartesian coordinates
D	rotor diameter		
E	energy fraction of POD mode	ζ_n	the eigenvectors
$f(x.nt)$	instantaneous flow field of snapshots	λ	tip speed ratio
k	azimuthal wave number	λ_n	the eigenvalues
N	the total number of snapshots	Ω	rotation speed
R	rotor radius	ω	vorticity
r	local radius	$\Phi_n(x)$	the eigenmodes
u	axial velocity		

1. INTRODUCTION

During the last decade, horizontal axis wind turbine has became a critical component of power generation in many countries over the world. For this reason, many researchers have focused their efforts on the aerodynamic optimization of the turbine rotor performance in particular the blade geometry and the wake structure.

The first attempt to evaluate the performance of an ideal wind turbine was conducted by Lanshester (1915). Afterwards, most developed tools involve the blade element momentum theory, which was originally introduced by Glauert (1935). This method is based on the aerodynamic performance assessment of a blade element under operational conditions. Consequently, empirical adjustment of experimental aerodynamic coefficients obtained from wind tunnel pressure measurement are generally recommended to take account of the local flow characteristics in the rotor region. Therefore, it is crucial to investigate on the rotor wake structure, which ultimately dictates the fluid loading on the wind turbine blades.

Owing to the high cost of experiments, a lack of experiments in this field was noticed (Vermeer *et al.* 2003). Furthermore, the accuracy of the obtained results is sensitive to many parameters such as the blockage ratio, the measurement technique and the recorded data quality.

In this context, many researchers have used the hot wire anemometry technique in the exploration of the wind turbine wake. Ebert and Wood (1997) have estimated the wind speed deficit in the near wake of a small horizontal axis wind turbine for different tip speed ratios. Vermeer and Van Bussel (1990) have conducted numerical and experimental investigation on the near wake of a wind turbine model with a diameter equal to 1.2 m. Fisichella (2001) has studied the tip vortices trajectories of a model wind turbine under twenty-seven different test conditions. Obtained results have permitted to improve the performance of an existing numerical tool based on the prescribed wake/thin-lifting surface method by reducing calculations time to 60%. Hu *et al.* (2007) have underlined the complexity of the wind turbine near wake for a horizontal axis wind turbine model tested in a circular cross-section wind tunnel.

Literature review indicated many other publications adopting the Particle Image Velocimetry (PIV) measurement technique for near wake analysis. Myers and Bahaj (2007) have tested a 0.4m diameter horizontal axis marine turbine in a circular water channel. The turbine performance and wake characteristics have been studied for three different velocities (1.55, 1.8 and 2.35 m/s). Whale *et al.* (2000) have compared the experimental vorticity maps and the numerical results obtained from the inviscid free-wake code (ROVLM) developed at the University of Stuttgart. Results have confirmed the capability of this tool in terms of wake boundary shape, downstream wake contraction and tip vortex pitch. Grant *et al.* (2000) have measured the trajectories of the tip vortex filament and its effect on the wake development under several turbine yaw and blade azimuth angle. In the European project MEXICO, Snel *et al.* (2007) have evaluated the tip vortex positions in the wake of a full-scale wind turbine for a tip speed ratio of 6.7. Sherry *et al.* (2013) have examined the stability of the helical vortex filaments downstream of a horizontal axis wind turbine and the interaction between the root and tip vortex. Massouh and Dobrev (2014) have performed a phase-locked PIV measurement in the near wake of a wind turbine to estimate the tip vortices circulation, the vortex core diameter and the peak tangential velocity for various vortex ages. Lignarolo *et al.* (2014) have studied the development of the wake flow structures for different tip speed ratio and the influence of the blade tip vortex in the wake re-energising process. Noura *et al.* (2016) have conducted an experimental and numerical investigation on the rotor wake of horizontal axis wind turbine under yawed condition.

The present paper aims to improve the database knowledge about the physical phenomena occurring in the near wake of a horizontal axis wind turbine. It reports on a set of experiments conducted in the subsonic wind tunnel of the Research and Technology Center of Energy (CRTEn) in Tunisia. The PIV technique was chosen to characterize the coherent structures downstream of a model wind turbine using the phase locked average method. A blockage ratio of 13.88 % was carefully selected to be suitable for the range of tip speed ratio considered in this study according to the recommendations of Sarlak *et al.* (2016). The tip vortex meandering phenomenon was analyzed using the Proper Orthogonal Decomposition (POD) method. The perturbations affecting this helical vortex filament were identified in each vortex sub-region, so that the influence of the other wake structures are minimized and the development of each perturbation are evaluated.

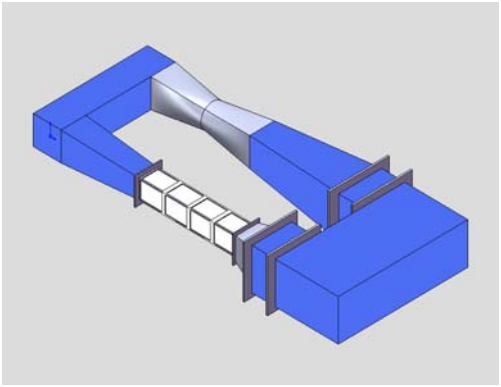

Fig. 1. CRTEn wind tunnel.

2. EXPERIMENTAL FACILITY

The experiments were carried out in the CRTEn subsonic wind tunnel characterized by a rectangular cross-section of 1000×800 mm² and a maximum wind speed equal to 30 m/s. It can be used in open or closed jet configuration (Fig.1) with a good stability and a turbulence intensity less than 0.1%, which represents optimal conditions for wind turbine tests. The wind turbine model was mounted on a metallic mast with the hub centered in the cross-section (Fig.2).

Fig. 2. Wind turbine in the center of the cross-section.

The three-bladed wind turbine model has been

designed to be suitable for experimentation in the wind tunnel of CRTEn. It has been equipped with a permanent magnet generator in order to estimate the power production. In addition, various blade support have been manufactured to allow the use of several blade geometries and the adjustment of the blade pitch within a wide range of angles (from 0° to 90°).

In this study, the blades have been made from Samba wood with a constant cord length and a fixed pitch angle in order to minimize the parameters affecting the near wake development. The diameter of the rotor is 376 mm and the blades have been manufactured based on the NACA 4412 airfoil with a constant chord length *c* equal to 50 mm and a constant pitch angle of 9.5° (Fig.3 and Fig.4).

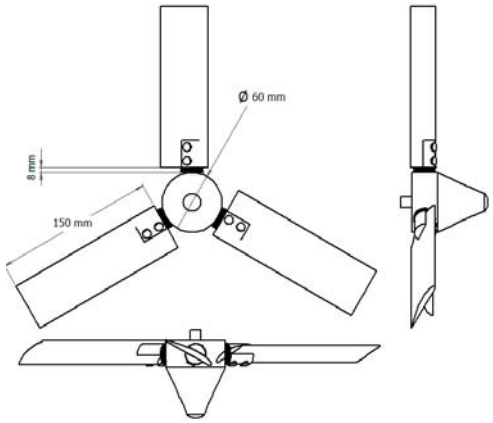

Fig. 3. Rotor of the model wind turbine.

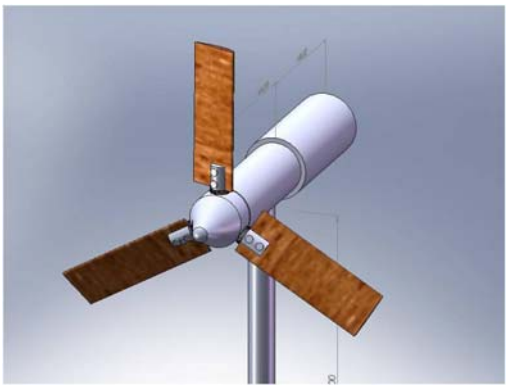

Fig. 4. Three dimensional views of the model wind turbine.

3. PIV MEASUREMENT SYSTEM

The PIV technique is a non-intrusive laser optical method of fluid visualization allowing instantaneous velocity measurements. The fluid is seeded with tracer particles that follow faithfully the flow dynamics. Therefore, the tracking of the particles displacement permits the fluid velocity calculation. The main advantage of the PIV is the generation of a bi-dimensional vector fields while other techniques allow a punctual velocity measurement.

The PIV system (Fig.5) used during the experiments was provided by Dantec Dynamics. It consists of:

1. A dual-pulsed Nd:YAG laser with 532 nm wavelength and 65 mJ energy output at 15 Hz of maximum frequency;
2. A FlowSense CCD camera with resolution up to 1600x1200 pixels;
3. A synchronizer acting as an external trigger for control of laser and CCD camera;
4. A high volume oil droplet-seeding generator;
5. The Dynamic Studio software V 2.40 for acquiring, storing and analyzing image based data;
6. An optical sensor for rotational speed measurement.

Fig. 5. PIV measurement system.

The Remote Optical Self-Powered Sensor SPSR 115/230 is used with a T5 reflective target fixed in a specific position on the model rotor to obtain a Transistor-Transistor Logic TTL signal for laser-triggering. The PIV acquisition starts when the reference signal is received in the specific BNC connector on the timer Box. The synchronization between laser shootings and azimuthally position permits us to deduce the average field of the instantaneous velocity for a rotor angle of 60°. During the experiments, the double frame mode is used to acquire images with a time delay set to 45µs.

4. PIV IMAGE PROCESSING

The PIV technique is a sensitive method for velocity measurement, so it is necessary to define the optimal experiment parameters in order to improve the quality of the recorded data. In this study, seven different tip speeds ratios $\lambda=\Omega R/V$ are investigated [3.50; 4.08; 4.27; 4.59; 4.81; 5.05; 5.22]. In each case, the camera captures 245 pairs of 10 bits 1600 by 1200 pixels images. The field of view (FOV) considered during PIV measurements is 272.4 × 204.3mm², which corresponds to a scale factor of 23.01. The statistical processing of the raw images is carried out through the Dantec Dynamic Studio v2.30.

The first step consists in processing the raw image to ameliorate the quality of the recorded data. Thus, the image-balancing module enables the adjustment of the non-uniformity in the light sheet, followed by the min, the max and the mean filters to enhance the image contrast.

In the second step, the adaptive correlation method was selected to calculate velocity vectors with a final interrogation area of 32×32 pixels and an overlapping of 50%, which corresponds to a spatial resolution of 2.72 mm. Then, the results were validated by the local median method and the average filter. False vectors in the exploration window were smoothed out by arithmetic averaging over the neighbor vectors.

Instantaneous velocity fields, resulting from each time series, give the average field in the investigated window. In addition, the processing of the calibrating image allows the deduction of the scale factor, the true velocity and the position of each structure relative to the rotor.

5. RAW IMAGE

The investigation plan used during the measurement of wind turbine near wake characteristics was selected carefully to minimize the laser light reflections as illustrated in the Fig.6.

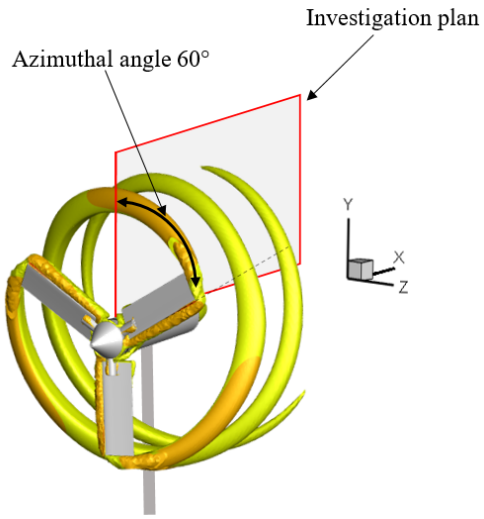

Fig. 6. PIV investigation plan.

Three core vortices downstream of the rotor are clearly distinguished in the Raw image obtained from the CCD camera (Fig.7). They represent the intersection between the helical tip vortex filaments and the exploration plan corresponding to vortex age 60°, 180° and 300°. In fact, the seeding particle density decreases in the tip vortex region due to the high values of the tangential velocity. As expected in the Rankine-Froude theory, we observe a slight expansion of the near wake.

The tip vortex locations for each pairs of images are illustrated in the Fig.8. It was noticed that the development of the helical tip vortex filaments downstream of the rotor is accompanied by an oscillation of vortex core position called vortex meandering. The amplitude of this phenomenon increases in the wake and mainly affects the characteristics of trailing vortices in the PIV averaged data. Therefore, it must be considered in the characterization of the vortex properties (Mula and Tinney 2014).

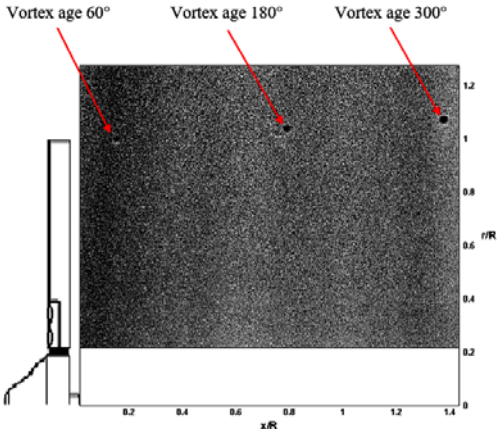

Fig. 7. Raw image (λ=3.50).

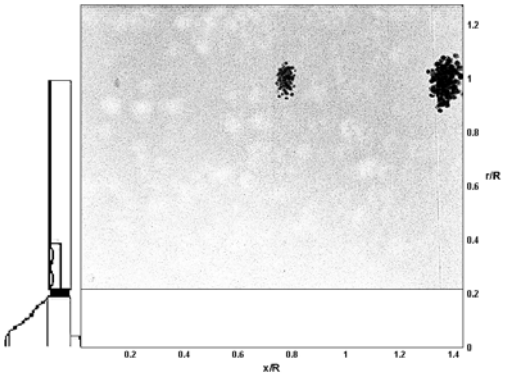

Fig. 8. Tip vortices position for 245 image pairs (λ=3.50).

6. CHARACTERISTICS OF PIV VELOCITY FIELD

Behind the wind turbine rotor, vortices are continuously generated in the wake from each blade trailing edge. A helicoidal sheet is progressively established downstream of the rotor and the wind turbine wake is developed. In addition, helical vortex filaments are observed on both root and tip regions, which move at the local flow velocity. Around each vortex, two important phenomena are distinguished: an acceleration of particles motion in the outer region of the wake and a slow down in the inner region. This change in particles dynamics behavior is due to the high value of the induced velocity generated near the tip and the root vortices as shown in Fig.9 for a tip speed ratio of λ=4.08.

Furthermore, a small increase of the wake tube diameter downstream of the rotor is observed. This result is in good agreement with the experimental

study conducted by Whale *et al.* (2000). They have affirmed that the wake expansion depends on the tip speed ratio and for lower values (λ=3-4) the radius of the wake tube remains approximately constant.

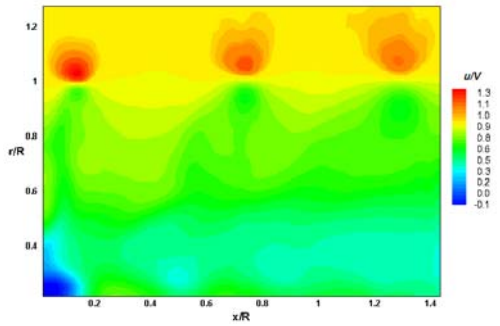

Fig. 9. The axial velocity field in the near wake.

7. ASPECTS OF WAKE VORTICITY

The wind turbine wake is very complex and difficult to predict because of swirling structures, which are organized movements on broad scale characterized by an important vorticity and a high-energy content. The identification of these coherent structures is crucial to understand the various physical phenomena observed in this region. Thus, it is recommended to follow their spatial and temporal fluctuations and to quantify energy losses in the wake.

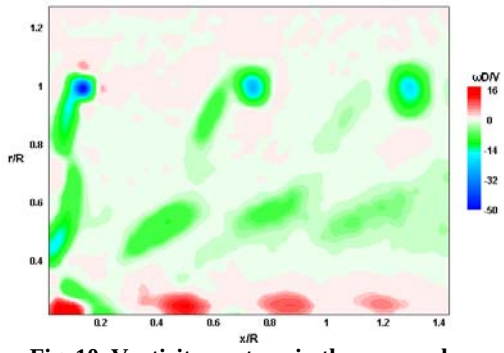

Fig. 10. Vorticity contour in the near wake.

The velocity information derived from PIV measurements was processed to draw the normalized vorticity map as shown in Fig.10. Four vortices are clearly located in the root region against three in the tip region in the exploration window, which can be explained by the progressive stretching of the helicoidal sheets related to high velocity gradient between the two regions. We also note a fast decrease of the root vortex strength due to the energy exchanges with other dissipative structures in the inner region.

For further understanding of the behavior of tip-vortex core in the wind turbine near wake, the axial and radial positions of each vortex were analyzed for different tip speed ratios.

The Fig.11a gives the mean axial positions of each tip vortex core for seven different tip speed ratios. It is apparent that the first vortex position is quasi-static over the experiment conditions. However, the other vortices move towards the rotor and the distance between them decreases when the tip speed ratio increases. The radial positions (Fig.11b) affirm the slight expansion of the near wake for all experiment cases. This phenomenon is more explicit when the tip speed ratio increases as assumed by Sherry *et al.* (2013).

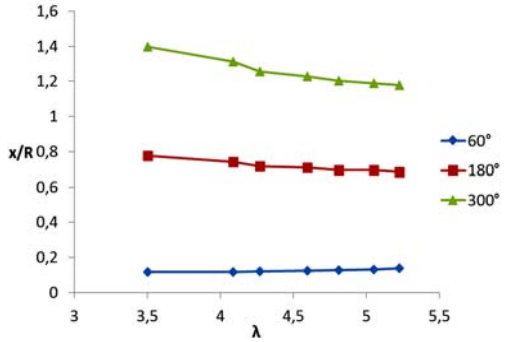

Fig. 11a. Tip vortex axial position.

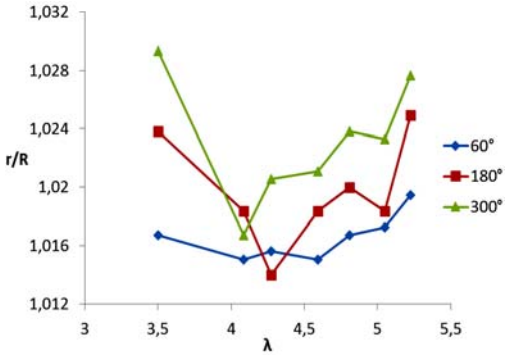

Fig. 11b. Tip vortex radial position.

In addition, the helical wake structure depends immediately on the core vortex local velocity essentially in the tip region. For this reason, the mean axial and radial velocities over the tip vortex age 60°, 180° and 300° were processed in Fig.12 and Fig.13 for λ=4.08. As shown, the core vortex radius increases gradually over the wake because of the radial stretching and the interactions with local instabilities. In fact, the axial speed in the core tip vortex decreases from 0,945 V for vortex age 60° to 0,886 V for vortex age 300° . As a result, the wake helical structure become progressively more unstable and the far wake meandering will eventually occurs (Machefaux *et al.* 2013).

8. POD ANALYSIS OF TIP VORTEX

POD analysis provides an important information about the perturbations affecting the development of the helical tip vortex filament in the wake of wind turbines. According to Faber *et al.* (2006) two different mechanisms were responsible for vortex meandering, which are the viscous instability affecting the vortex core and the energy exchange

with others external instabilities. Many papers have used this technique to understand different phenomena observed in the wake of wind turbine (Premaratne *et al.* 2016, Bastine *et al.* 2014, Aloui *et al.* 2013 and Larsen *et al.* 2007). The Proper Orthogonal Decomposition (POD) is a mathematical technique used to identify the dominant structures in the fluid flows by linear decomposition and reconstruction. The elementary idea of POD is to define a set of orthogonal functions (eigenmodes) with random coefficients representing the field based on an energy-weighted calculation. The eigenmodes are sort in descending order according to their energy content (eigenvalues). Therefore, this method provides an efficient process of low-order reconstruction of fluid flow structures with the desired precision using a suitable number of modes.

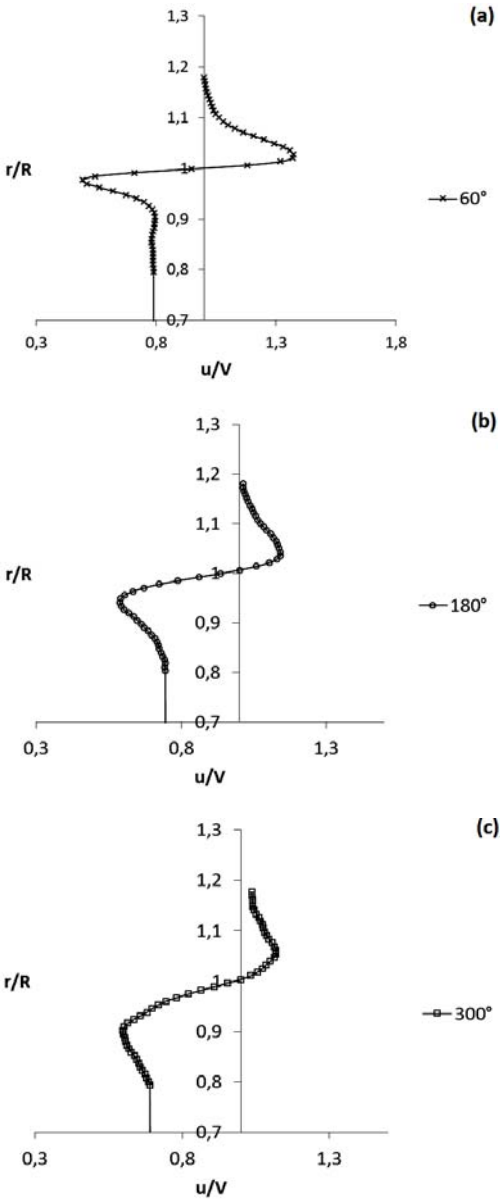

Fig. 12. Axial tip vortex velocity: (a) vortex age 60°, (b) vortex age 180° and (c) vortex age 300°.

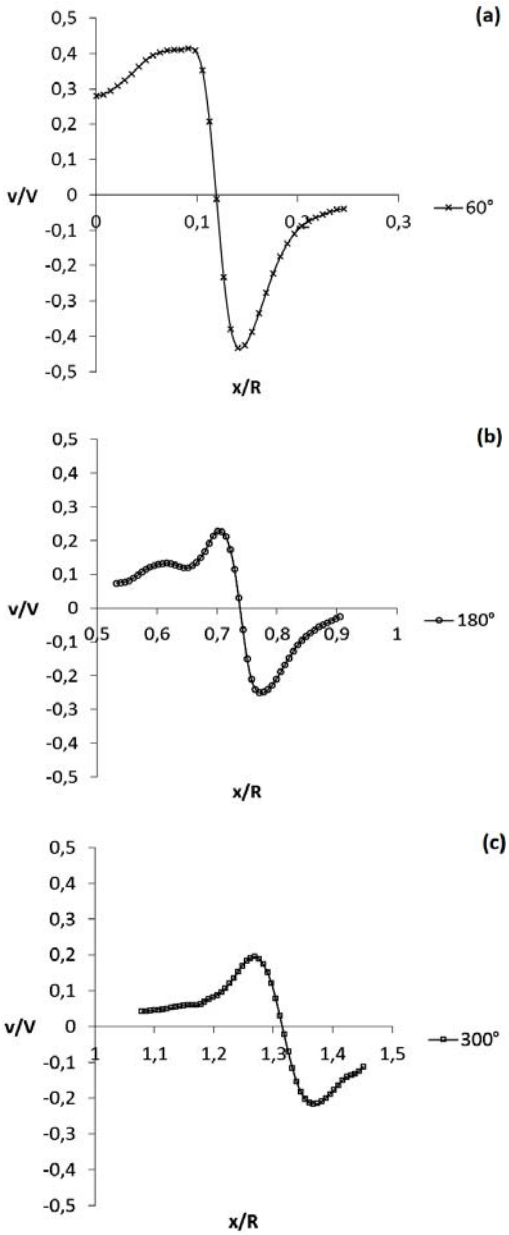

Fig. 13. Radial tip vortex velocity: (a) vortex age 60°, (b) vortex age 180° and (c) vortex age 300°.

In this paper, the snapshot POD method is adopted. It consists in expressing the studied functions $f(x)$ in terms of eigenmodes and can expressed as follow:

$$f_n(x) = \sum_{n=1}^{N} a_n \Phi_n(x) \tag{1}$$

With $f_n(x) = f(x,nt)$ is the instantaneous velocity field of snapshots and N is the total number of snapshots. Since the eigenmodes $\Phi_n(x)$ are orthonormal, the respective a_n coefficients modes are uncorrelated:

$$\langle a_n , a_m \rangle = \lambda_n \delta_{nm} \tag{2}$$

Where the angled brackets denote the ensemble-averaging operator. The eigenvalue λ_n represents the contribution of the corresponding eigenmodes $\Phi_n(x)$

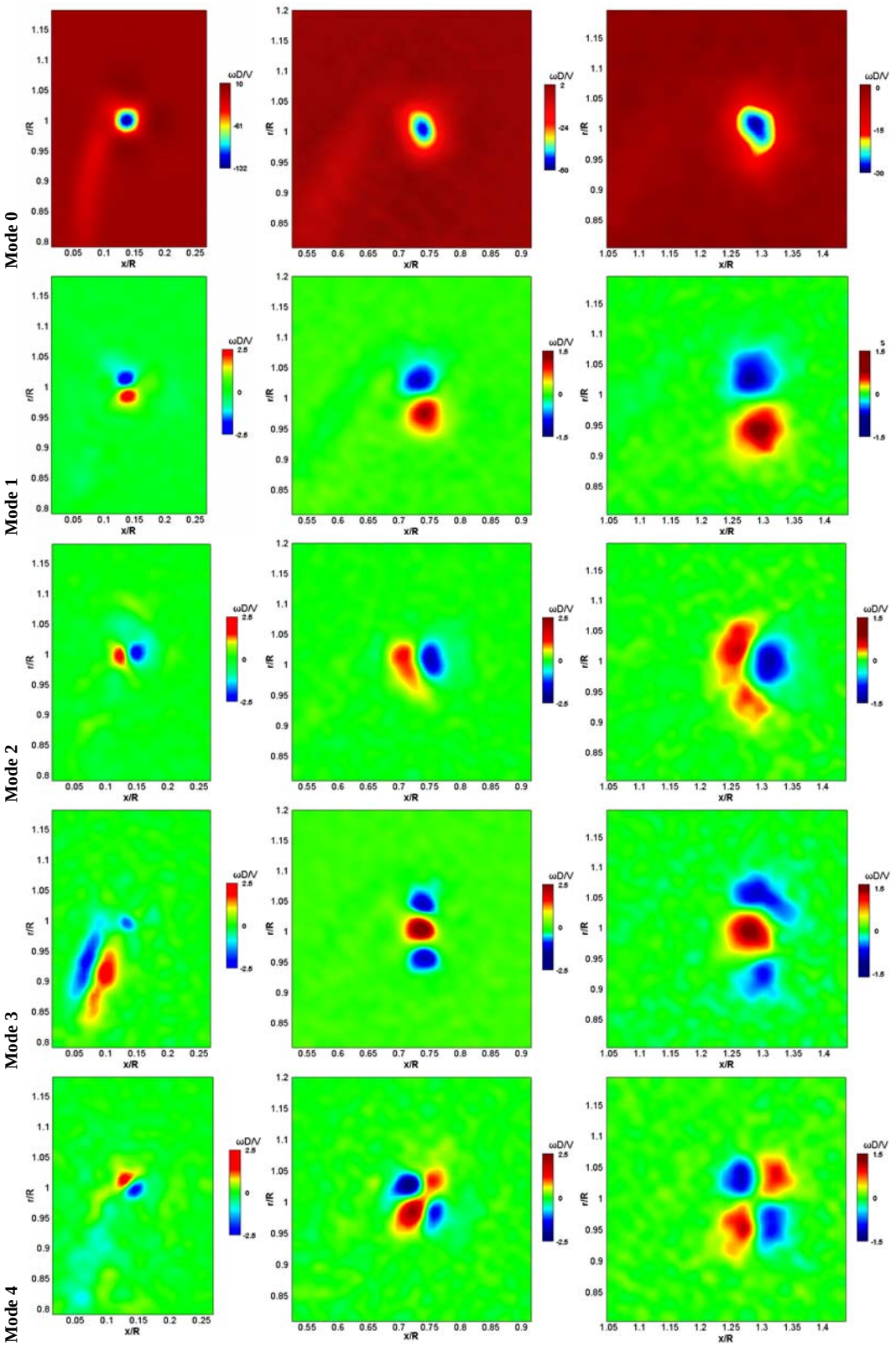

Fig. 14. POD modes 0 to 4. (Left vortex age 60°, middle vortex age 180° and right vortex age 300°).

to the total energy. According to Bastine *et al.* (2014), the eigenmodes are calculated as follow:

$$\Phi_n(x) = \sum_{n=1}^{N} \zeta_n f_n(x) \tag{3}$$

ζ_n are the eigenvectors of the spatial correlation matrix C that is defined by the inner product of the velocity fields at times n and m:

$$C_{nm} = \frac{1}{N}(f_n, f_m) \tag{4}$$

The POD is an efficient mathematical method for fluid dynamics study. However, the interpretation of results requires a good knowledge in the field of fluid mechanics. In order to understand the tip vortex meandering phenomenon, the velocity fields in each vortex sub-region were processed for λ=4.08 using a final interrogation area of 16×16 pixels and an overlapping of 50%. Fig. 14 represents the POD modes obtained from analysis of the fluctuating part of velocity field in the studied tip vortex region for 245 snapshots.

The first mode presents two axisymmetric contra-rotating structures organized in the radial direction, which corresponds to a Kelvin wave of an azimuthal wavenumber k=1 (Fabre, 2006). The main effect of these structures of opposite signs is to increase the vorticity in one part of the core vortex, and to decrease it in the other part. The consequence is a displacement of the whole vortex core in the imposed direction. Therefore, it is adequate to associate the first mode with the radial tip vortex oscillation. The energy fraction of the first mode rises progressively from the first to the third tip vortex as shown in Fig.15. Thus the intensity of radial oscillation phenomenon increases gradually providing a more unstable wake and contributes to the total wake meandering.

The second POD mode shows also two counter-rotating structures, which presents the axial oscillation of the core vortex due to the meandering phenomenon. The energy fraction of this mode increases during the wake development but it remains less important than the first one. This finding did not match the results obtained by Del Pino *et al.* (2011) for the non-rotating blade case. The combination of the first and the second mode characterizes the vortex motion in the axial and the radial directions.

The third and the fourth mode with an azimuthal wavenumber k=2, illustrate the elliptical deformations of the vortices due to the interaction with local structures in the wake. The energy fraction of the other modes are less significant and they are not considered in this work.

Low order reconstructions of the instantaneous velocity fields in the time step t= 11,525 s is also processed for the vortex age 180° using the first four modes. The Normalized vorticity is used to quantify the influence of each mode in the step-by-step reconstruction. A comparison between the reconstructed map and the instantaneous vorticity map confirms the ability of POD to identify the most important perturbation affecting the helical vortex filament.

As can be observed in the Fig.16, the vorticity increases with the addition of each fluctuation mode. The first reconstruction covers 33% of the total energy and affects essentially the radial position of the core vortex that has been moved from 0.796 R to 0.808 R. The addition of the second fluctuating mode induces a displacement of core vortex in the axial direction from 0.738 R to 0.727 R. The mode 3 and 4 are clearly responsible for the elliptical deformation of vortex structure as confirmed by Mula and Tinney (2014) in the case of a propeller rotor.

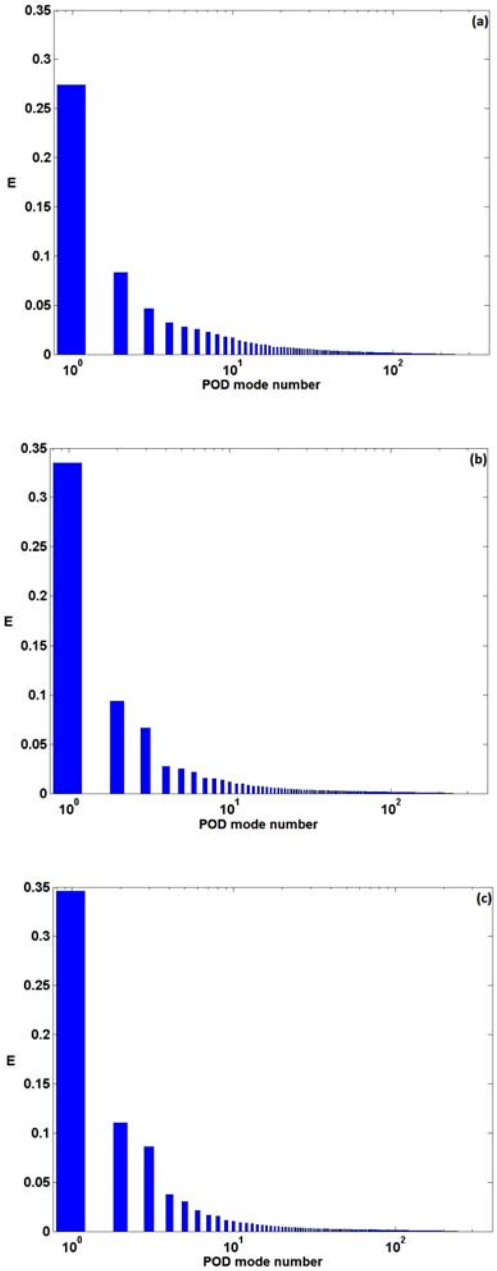

Fig. 15. Modal energy distribution: (a) vortex age 60°, (b) vortex age 180° and (c) vortex age 300°.

9. CONCLUSION

In this paper, we have conducted a series of wind tunnel measurements focused on the meandering

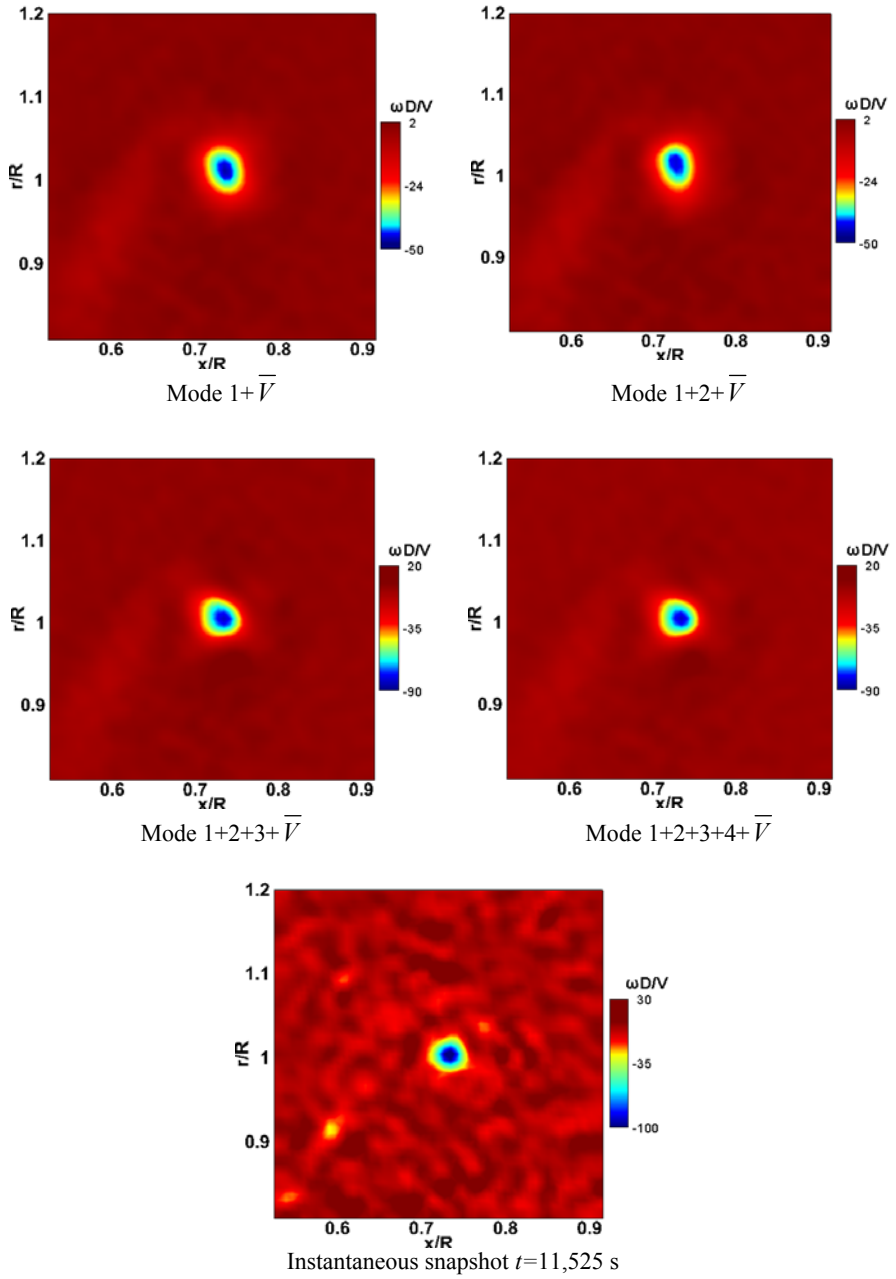

Fig. 16. Low order reconstructions of the instantaneous vorticity map.

characteristics of tip vortex in near wake of a horizontal axis wind turbine. The PIV technique allowed us to investigate on the perturbations affecting the helical tip vortex filament downstream of a three bladed rotor.

The PIV images processing shows a slight expansion of the wake for lower values of tip speed ratio and confirms that tip and root vortices are the main sources of energy loses in the wind turbine wake. The identification of core vortex positions prove that wandering phenomenon is a critical factor affecting the coherent structures arrangement downstream of the rotor.

The POD analysis of the velocity fields in each tip vortex sub-region led us to conclude that:

- The first mode, which represents the radial meandering, is the most energetic source of perturbation in each tip vortex region with about 1/3 of the total energy.
- The superposition of the first and the second modes illustrates the tip vortex meandering in the wind turbine near wake.
- The meandering phenomenon amplitude increases during the wake development giving a more unstable wake.

The further study will focus on the influence of other geometric parameters in the vortex meandering stability such as tip speed ratio, chord length and twist angle along the blade.

IN MEMORY OF PROFESSOR SASSI BEN NASRALLAH

We would like to pay tribute to our dear Professor Sassi BEN NASRALLAH, co-author of this paper, who left us suddenly on June 2017. Professor Sassi BEN NASRALLAH was for us an excellent teacher, a serious person and a scientific luminary. We lost more than just a colleague, but a scientific father.

REFERENCES

Aloui, F., M. Kardous, R. Cheker and S. Ben Nasrallah (2013). Study of the wake induced by a porous disc. In *Proceedings of the 21st French Congress of Mechanics CFM2013*, Bordeaux, France.

Bastine, D., B. Witha, M. Wächter and J. Peinke (2014). POD analysis of a wind turbine wake in a turbulent atmospheric boundary layer. *Journal of Physics: Conference Series* 524(1), 012153.

Del Pino, C., J. M. Lopez-Alonso, L. Parras, and R. Fernandez-Feria (2011). Dynamics of the wing-tip vortex in the near field of a NACA 0012 aerofoil. *The Aeronautical Journal* 115(1166), 229-239.

Fabre, D., D. Sipp and L. Jacquin (2006). Kelvin waves and the singular modes of the Lamb–Oseen vortex. *Journal of Fluid Mechanics* 551, 235-274.

Fisichella, C. J. (2001). *An Improved Prescribed Wake Analysis for Wind Turbine Rotors*. Ph. D. thesis, the University of Illinois, Champaign, USA.

Glauert H. (1935). Windmills and Fans, In W. F. Durand (Ed), *Aerodynamic theory*. Berlin, Julius Springer.

Grant, I., M. Mo, X. Pan, P. Parkin, J. Powell, H. Reinecke, K. Shuang, F. Coton and D. Lee (2000). An experimental and numerical study of the vortex filaments in the wake of an operational, horizontal-axis, wind turbine. *Journal of Wind Engineering and Industrial Aerodynamics* 85(2), 177-189.

Hu, D., J. Ren and Z. Du (2007). A measurement of the three-dimensional near-wake velocity field of a model horizontal-axis wind turbine, In K. Cen, Y. Chi and F. Wang (Eds), *Challenges of Power Engineering and Environment*. Berlin Heidelberg, Springer.

Lanchester, F. W. (1915). A contribution to the theory of propulsion and the screw propeller. *Naval Engineers Journal* 27(2), 509-510.

Larsen, G. C., H. Madsen Aagaard, F. Bingöl, J. Mann, S. Ott, J. N. Sørensen and *et al.* (2007). *Dynamic wake meandering modeling*. Risø National Laboratory for Sustainable Energy, Technical University of Denmark. Report number: Risoe-R: No. 1607(EN). ISSN 0106-2840 ISBN 978-87-550-3602-4

Lignarolo, L. E. M., D. Ragni, C. Krishnaswami, Q. Chen, C. S. Ferreira and G. J. W. Van Bussel (2014). Experimental analysis of the wake of a horizontal-axis wind-turbine model. *Renewable Energy* 70, 31-46.

Machefaux, E., G. C. Larsen, N. Troldborg, M. Gaunaa and A. Rettenmeier, (2015). Empirical modeling of single‐wake advection and expansion using full‐scale pulsed lidar‐based measurements. *Wind Energy* 18(12), 2085-2103.

Massouh, F. and I. Dobrev (2014). Investigation of wind turbine flow and wake. *Journal of Fluid Science and Technology* 9(3), JFST0025-JFST0025.

Mula, S. M., and C. E. Tinney (June 2014). Classical and snapshot forms of the POD technique applied to a helical vortex filament. *44th AIAA Fluid Dynamics Conference,* Atlanta, Georgia, USA.

Myers, L. and A. S. Bahaj (2007). Wake studies of a 1/30th scale horizontal axis marine current turbine. *Ocean Engineering* 34(5), 758-762.

Noura, B., I. Dobrev, R. Kerfah, F.Massouh and S. Khelladi (2016). Investigation of the Rotor Wake of Horizontal Axis Wind Turbine under Yawed Condition. *Journal of Applied Fluid Mechanics* 9(6), 2695-2705.

Premaratne, P., W. Tian and H. Hu (June 2016). Analysis of Turbine Wake Characteristics using Proper Orthogonal Decomposition (POD) and Triple Decomposition. *46th AIAA Fluid Dynamics Conference*, Washington, D.C. USA.

Sarlak, H., T. Nishino, L. A. Martínez Tossas, C. Meneveau and J. N. Sørensen (2016). Assessment of blockage effects on the wake characteristics and power of wind turbines. *Renewable Energy* 93, 340-352.

Sherry, M., J. Sheridan and D. L. Jacono (2013). Characterisation of a horizontal axis wind turbine's tip and root vortices. *Experiments in Fluids* 54(3), 1417.

Snel, H., J. G. Schepers and B. Montgomerie (2007). The MEXICO project (Model Experiments in Controlled Conditions): The database and first results of data processing and interpretation. *Journal of Physics: Conference Series* 75(1), 012014.

Vermeer, L. J., J. N. Sørensen and A. Crespo (2003). Wind turbine wake aerodynamics. *Progress in Aerospace Sciences* 39(6), 467-510.

Vermeer, N. J. and G. J. W. Van Bussel (1990). Velocity measurements in the near wake of a model rotor and comparison with theoretical results. In *Proceedings of the European*